

Oscillatory dynamics of the classical Nonlinear Schrodinger equation

D.S. Agafontsev^(a), V.E. Zakharov^{(a),(b),(c)}

^(a) *P. P. Shirshov Institute of Oceanology, 36 Nakhimovsky prosp., Moscow 117218, Russia*

^(b) *L. D. Landau Institute for Theoretical Physics, 2 Kosygin str., 119334 Moscow, Russia*

^(c) *Department of Mathematics, University of Arizona, Tucson, AZ, 857201, USA*

We study numerically the modulation instability (MI) developing from a condensate solution seeded by weak noise in the framework of the classical (integrable) one-dimensional Nonlinear Schrodinger (NLS) equation. We demonstrate that in the nonlinear stage of the MI the averaged over ensemble of initial data *generalized means* (or *power means*) of the solutions amplitudes oscillate with time around their asymptotic values very similar to sinusoidal law; the amplitudes of these oscillations decay with time t as $t^{-3/2}$, the phases of these oscillations contain nonlinear phase shift that decays as $t^{-1/2}$, and the period of the oscillations is equal to π . The asymptotic values of the experimental generalized means coincide with the generalized means corresponding to Rayleigh probability density function (PDF) of waves amplitudes appearance. The same behavior is also shown for the PDF of waves amplitudes. We study how these oscillations depend on the initial noise properties and demonstrate that they should be visible for a very wide variety of statistical distributions of noise.

I. INTRODUCTION.

The problem of the modulation instability (MI) was first discovered by T.B. Benjamin and J.E. Feir in 1967 for periodic surface gravity waves [1] and since then remains one of the most difficult and interesting problems of mathematical physics. In 1968 V.E. Zakharov [2] came independently to the same results and demonstrated that the instability observed in [1] using direct surface shape equations was in fact the manifestation of the MI of a condensate solution

$$\Psi = C e^{i\gamma|C|^2 t}, \quad (1)$$

for the classical one-dimensional Nonlinear Schrodinger (NLS) equation of focusing type,

$$i\Psi_t + \beta\Psi_{xx} + \gamma|\Psi|^2\Psi = 0. \quad (2)$$

Here t is time, x is spacial coordinate, β and γ are real nonzerth coefficients so that $\beta\gamma > 0$, and Ψ is wave field envelope.

Today the classical NLS equation is recognized as a universal model equation describing the evolution of the envelope of quasimonochromatic wave train in weakly nonlinear media [3]. It has a vast number of applications from surface water waves and propagation of light pulses to Bose-Einstein condensate theory and plasma waves [2, 4–7]. The evolution of its simplest condensate solution during the MI, however, is still under discussion [8].

Let us suppose that

$$\Psi|_{t=0} = C + \epsilon(x)$$

is the initial condensate state (1) seeded by small noise $|\epsilon(x)| \ll |C|$. After the scaling and gauge transformations $x = \tilde{x}\sqrt{\beta/(\gamma|C|^2)}$, $t = \tilde{t}/(\gamma|C|^2)$, $\Psi = C\tilde{\Psi}e^{i\tilde{t}}$ and $\epsilon = C\tilde{\epsilon}e^{i\tilde{t}}$, the problem of the evolution of this state is reduced to

$$i\Psi_t - \Psi + \Psi_{xx} + |\Psi|^2\Psi = 0, \quad \Psi|_{t=0} = 1 + \epsilon(x), \quad (3)$$

where all tilde signs are omitted. In terms of Eq. (3), the MI develops on the background of the exact condensate solution $\Psi = 1$, amplifying small periodic modulations

$$\Psi = 1 + \kappa \exp(ikx + i\Omega t), \quad \Omega^2 = k^4 - 2k^2,$$

for wavenumbers $k \in (-\sqrt{2}, \sqrt{2})$, and the maximum increment of the instability is realized at $|k| = k_0 = 1$. When these modulations are small, their evolution can be effectively described by the linearized equations [2], and the corresponding stage of the MI is called linear one. As the modulations grow, the linearization no longer works and the full classical NLS equation is necessary. This corresponds to nonlinear stage of the MI.

In the current publication we demonstrate the oscillatory dynamics of the classical NLS equation in the nonlinear stage of the MI. The first indication for this was in fact obtained in [9], where the statistical properties of the MI development were studied. Namely, it turned out that the averaged over ensemble of initial data kinetic and potential energy regularly oscillate with time around their asymptotic values, and the amplitude of these oscillations decays as time increases. Initial data of the ensemble corresponded to the condensate state $\Psi = 1$ seeded by small noise; the statistical properties of noise were fixed and the realization of noise varied within the ensemble. The similar behavior was also shown for the probability density function (PDF) of waves amplitudes appearance.

Here we continue this study. We demonstrate that in the nonlinear stage of the MI the ensemble average *generalized means* (or *power means*) $M^{(n)}(t)$ of the amplitudes $|\Psi(x, t)|$ with exponents $n \neq 2$ oscillate with time around their asymptotic values $M_A^{(n)}$ very similar to sinusoidal law, while the amplitudes of these oscillations decay with time as $t^{-3/2}$. Also, the phases of these oscillations contain nonlinear phase shift that decays as $t^{-1/2}$, and the period of the oscillations is equal to π . Under the gener-

alized means $M^{(n)}(t)$ we understand

$$\begin{aligned} M^{(n)}(t) &= \left\langle \frac{1}{L} \int_{-L/2}^{+L/2} |\Psi(x, t)|^n dx \right\rangle^{1/n} = \\ &= \left(\int_0^{+\infty} |\Psi|^n P(|\Psi|, t) d|\Psi| \right)^{1/n}, \end{aligned} \quad (4)$$

where $\langle \dots \rangle$ stands for averaging over ensemble of initial data, $L = \int dx$ is the length of the integration region and $P(|\Psi|, t)$ is the PDF to meet amplitude $|\Psi|$ at time t . We prove that the asymptotic values $M_A^{(n)}$ of the generalized means $M^{(n)}(t)$, around which the oscillations occur, coincide with the values $M_R^{(n)}$ of the generalized means corresponding to purely Rayleigh PDF $P_R(|\Psi|)$. We also demonstrate the same behavior for the PDFs $P(|\Psi|, t)$ for not very large amplitudes $|\Psi|$ beyond which our methods do not provide reliable results. Then we examine how the oscillations we observe depend on the statistical properties of initial noise.

II. NUMERICAL METHODS.

We integrate Eq. (3) numerically in the box $-128\pi \leq x < 128\pi$ with periodic boundary over the period of time $t \in [0, 200]$. We start from initial data $\Psi|_{t=0} = 1 + \epsilon(x)$ where $|\epsilon(x)| \ll 1$ is statistically uniform in space stochastic noise,

$$\epsilon(x) = A_0 \left(\frac{L\sqrt{8\pi}}{\theta} \right)^{1/2} \int e^{-k^2/\theta^2 + i\xi_k + ikx} \frac{dk}{2\pi}, \quad (5)$$

A_0 is noise amplitude, $L = 256\pi$ is the length of the integration region, θ is noise width in k-space, and ξ_k are arbitrary phases for each k . The average squared amplitude of noise in x-space can be calculated as,

$$\begin{aligned} |\overline{\epsilon}|^2 &= \frac{\int |\epsilon|^2 dx}{\int dx} = \frac{L\sqrt{8\pi}}{\theta} \frac{A_0^2}{L} \times \\ &\times \int e^{-(k_1^2 + k_2^2)/\theta^2 + i(\xi_{k_1} - \xi_{k_2}) + i(k_1 - k_2)x} \frac{dk_1 dk_2}{(2\pi)^2} dx \approx \\ &\approx A_0^2. \end{aligned} \quad (6)$$

Below we will concentrate on the experiment with $A_0 = 10^{-5}$, $\theta = 5$; such noise in the range of the MI $k \in (-\sqrt{2}, \sqrt{2})$ can be treated as a white noise. Then we will demonstrate comparison with the experiments with different values of A_0 and θ . Note that in [9] the smaller integration region was used, $L = 32\pi$. In this publication we had to use $L = 256\pi$ because we found that on the period of time $t \in [0, 200]$ the oscillations we observe depend on L if $L < 128\pi$.

We use Runge-Kutta 4th-order method. In order to improve simulations and save computational resources we employ adaptive change of the spacial grid size Δx reducing it when Fourier components of the solution Ψ_k at high wave numbers k exceed $10^{-13} \max |\Psi_k|$ and increasing Δx when this criterion allows. In order to prevent

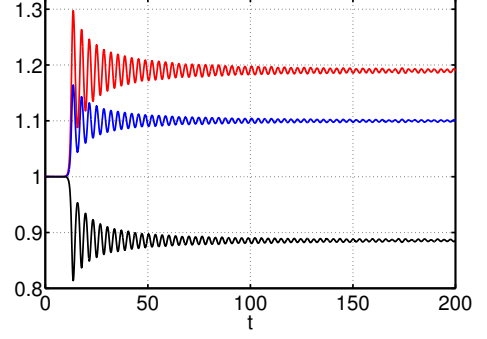


FIG. 1. (Color on-line) Evolution of the generalized means $M^{(1)}(t)$ (black), $M^{(3)}(t)$ (blue) and $M^{(4)}(t)$ (red). Ensemble of initial data was generated with noise parameters $A_0 = 10^{-5}$, $\theta = 5$.

appearance of numerical instabilities, time step Δt also changes with Δx as $\Delta t = h\Delta x^2$, $h \leq 0.1$. For most of the simulations we use ensembles of 1000 initial distributions each. We checked our statistical results against the size of the ensembles and implementation of other numerical methods (Runge-Kutta 5th order and Split-Step 2nd and 4th order methods [10, 11]) and found no significant difference.

III. OSCILLATORY BEHAVIOR.

FIG. 1 shows oscillations of the generalized means $M^{(n)}(t)$ with exponents $n = 1$, $n = 3$ and $n = 4$. The generalized mean with exponent $n = 2$ does not oscillate, $M^{(2)}(t) \approx 1$, because $M^{(2)} = \sqrt{\langle N \rangle / L}$ where

$$N = \int_{-L/2}^{+L/2} |\Psi(x, t)|^2 dx$$

is wave action that is conserved by the classical NLS equation; $\langle N \rangle \approx L$ since $\Psi|_{t=0} = 1 + \epsilon(x)$ and $|\epsilon(x)| \ll 1$. For $n \neq 2$ oscillations start in the nonlinear stage of the MI at $t \sim 12$; $M^{(n)}(t)$ for $n \geq 3$ oscillate in-phase so that the positions of their minimums and maximums coincide, and antiphase with $M^{(1)}(t)$ so that the positions of minimums of $M^{(1)}(t)$ coincide with the positions of maximums of $M^{(n)}(t)$, $n \geq 3$, and vice versa.

As was demonstrated in [9], the PDF $P(|\Psi|, t)$ for the classical NLS equation is close to Rayleigh one, especially at large times. For a purely Rayleigh PDF,

$$P_R(|\Psi|) = \frac{2|\Psi|}{\sigma^2} \exp(-|\Psi|^2/\sigma^2), \quad (7)$$

the corresponding generalized means can be readily calculated. Indeed, Eq. (4) yields

$$M_R^{(n)} = \left(\frac{2}{\sigma^2} \int_0^{+\infty} |\Psi|^{n+1} \exp(-|\Psi|^2/\sigma^2) d|\Psi| \right)^{1/n}, \quad (8)$$

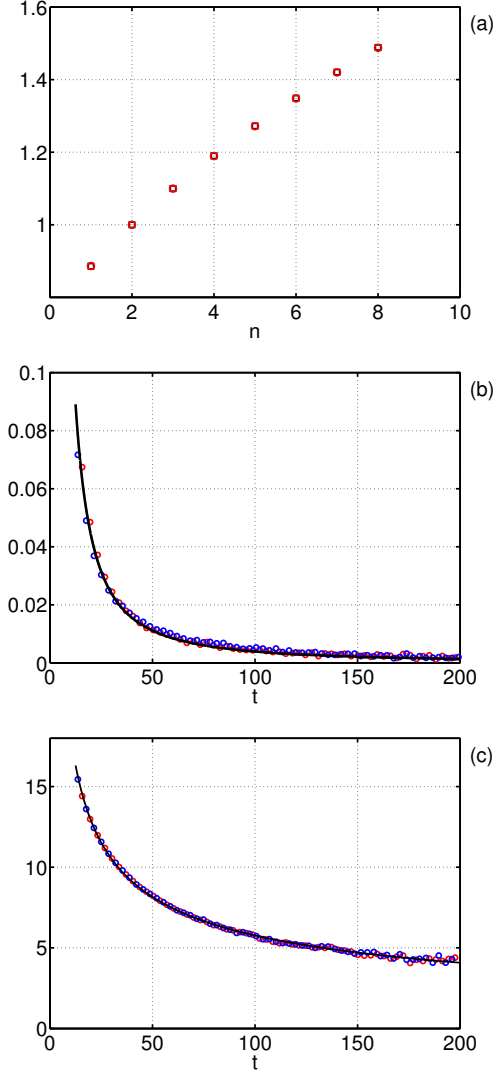


FIG. 2. (Color on-line) Graph (a): asymptotic values $M_A^{(n)}$ of the generalized means around which the oscillations occur, calculated by averaging $M^{(n)}(t)$ over time $t \in [150, 200]$ (black squares), and their predictions based on Rayleigh PDF $M_R^{(n)}$ (9) (red circles), depending on exponent n for $n = 1, \dots, 8$. Graphs (b): amplitude of the oscillations of $M^{(1)}(t)$ calculated as the deviations of the extremums of $M^{(1)}(t)$ from $M_A^{(1)}$, depending on time t . Graph (c): nonlinear phase shift (11) calculated at the extremums of $M^{(1)}(t)$, depending on time t . On graphs (b) and (c) red circles mark local maximums, and blue circles - local minimums of $M^{(1)}(t)$. Black curve on graph (b) is fit by function $a/t^{3/2}$, $a \approx 3.94$, on graph (c) is fit by function c/\sqrt{t} , $c \approx 57.7$. Ensemble of initial data was generated with noise parameters $A_0 = 10^{-5}$, $\theta = 5$.

and the condition $M^{(2)} = 1$ gives $\sigma = 1$, therefore

$$M_R^{(n)} = (2I_{n+1})^{1/n}, \quad (9)$$

where

$$I_m = \int_0^{+\infty} x^m \exp(-x^2) dx.$$

FIG. 2a shows, depending on exponent n , the asymptotic values of the generalized means $M_A^{(n)}$ around which the oscillations occur, that were calculated by averaging $M^{(n)}(t)$ over time $t \in [150, 200]$, and also the values of their theoretical predictions $M_R^{(n)}$ (9) based on Rayleigh PDF (7) with $\sigma = 1$. The perfect coincidence of these results supports one of the conclusions of [9] that the PDF for the classical NLS equation coincides to Rayleigh one at large times. In this sense the oscillations of the generalized means $M^{(n)}(t)$ can be represented as the consequence of the fluctuations of the PDF near the Rayleigh shape (7) with $\sigma = 1$.

The amplitude of the oscillations of the generalized means, that we measure as the deviations of the local maximums and minimums of $M^{(n)}(t)$ from the asymptotic value $M_A^{(n)}$, decays with time as $a/t^{3/2}$, as shown on FIG. 2b. For our experiment with noise parameters $A_0 = 10^{-5}$, $\theta = 5$, the prefactor is equal to $a = (3.94 \pm 0.03)$ for $n = 1$.

It turns out that the period of the oscillations changes from $\Delta T \sim 4$ at $t \sim 20$ to $\Delta T \sim 3$ at $t \sim 200$. We think that this is the effect analogous to the nonlinear phase shift. Indeed, one can search for the approximation of $M^{(n)}(t)$ in the form

$$f(t) = M_A^{(n)} + \frac{a}{t^{3/2}} \sin(bt + \phi_{nl}(t) + \phi_0), \quad (10)$$

where the nonlinear phase shift $\phi_{nl}(t)$ should be proportional to the amplitude of the oscillations $a/t^{3/2}$ multiplied by time t , or $\phi_{nl}(t) = c/\sqrt{t}$ where c is constant. Then, the phases for the local maximums t_{max} of $M^{(n)}(t)$ should be equal to

$$\Phi_{max}(t_{max}) = bt_{max} + \frac{c}{\sqrt{t_{max}}} + \phi_0 = \frac{\pi}{2} + 2\pi m,$$

and for the local minimums t_{min} - to

$$\Phi_{min}(t_{min}) = bt_{min} + \frac{c}{\sqrt{t_{min}}} + \phi_0 = \frac{3\pi}{2} + 2\pi m,$$

where m is integer number. We find all the subsequent extremums t_{max} and t_{min} of $M^{(n)}(t)$ from one hand, and their phases Φ from the other hand by setting $m = 0$ for the first maximum, $m = 1$ for the second maximum, and so on. Then, with the help of the least squares method we determine the coefficients b , c and ϕ_0 , that in case of $n = 1$ are equal to $b = 1.99$, $c = 57.7$ and $\phi_0 = -44.1$. After that we check that the nonlinear phase shift

$$\Phi(t) - bt - \phi_0, \quad (11)$$

calculated at the extremums of $M^{(1)}(t)$, is indeed very well approximated by the function c/\sqrt{t} , as shown on FIG. 2c.

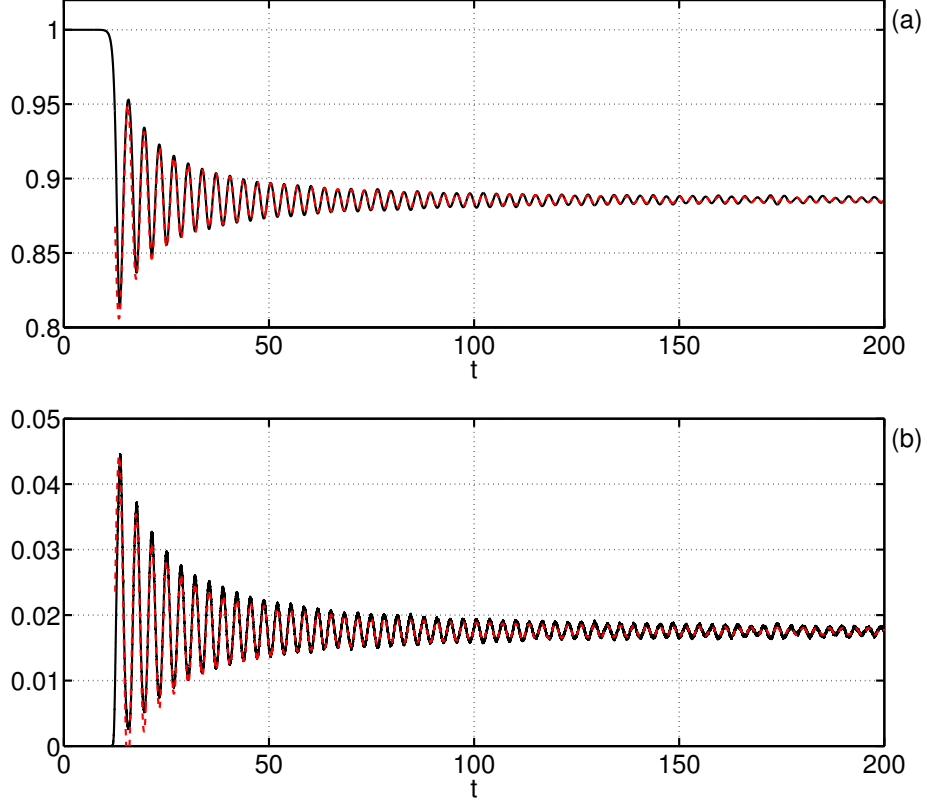


FIG. 3. (Color on-line) Evolution of the generalized mean $M^{(1)}(t)$ (a) and the squared amplitude PDF $P(|\Psi|^2, t)$ at $|\Psi|^2 = 4$ (b). Dashed red curves are fits by function $f(t) = f_0 + [a/t^{3/2}] \sin(bt + c/\sqrt{t} + \phi_0)$ with parameters $f_0 = 0.886$, $a = 3.94$, $b = 1.99$, $c = 57.7$, $\phi_0 = -44.1$ for graph (a) and $f_0 = 0.0175$, $a = 1.32$, $b = 1.99$, $c = 57.7$, $\phi_0 = -44.1 + \pi = -41$ for graph (b). Ensemble of initial data was generated with noise parameters $A_0 = 10^{-5}$, $\theta = 5$.

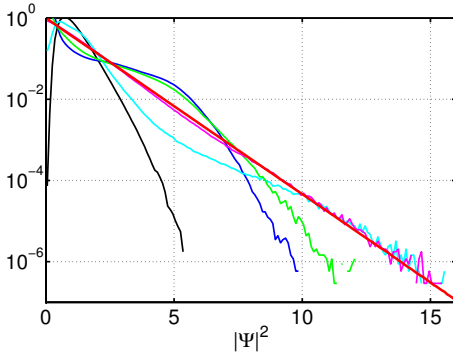


FIG. 4. (Color on-line) Ensemble average PDFs $P(|\Psi|^2)$ for squared amplitude $|\Psi|^2$ at $t = 12$ (black), $t = 14$ (blue), $t = 16$ (cyan), $t = 18$ (green), $t = 100$ (pink) and the asymptotic PDF calculated by averaging the PDF over time $t \in [150, 200]$ (thick red curve). The asymptotic PDF coincides with the exponent $\exp(-|\Psi|^2)$. Ensemble of initial data was generated with noise parameters $A_0 = 10^{-5}$, $\theta = 5$.

In our experiments we observe that the anzats (10) fits remarkably well to the experimental data for all generalized means $M^{(n)}(t)$, $n \neq 2$, that we measure. The

example of such fit for $M^{(1)}(t)$ is shown on FIG. 3a. The absence of the nonlinear phase shift (equivalent to $c = 0$), or the nonlinear phase shift with exponent different from -0.5 , leads to the situation when the anzats (10) does not fit to the oscillations, or fits significantly worse. It is interesting to note that the period of our oscillations $2\pi/b \approx 3.16$ is almost equal to π . We think that it should coincide with π since we measure the same period for all of our experiments.

In addition to the generalized means $M^{(n)}(t)$ we measure the probability density function $P(|\Psi|^2, t)$ to meet squared amplitude $|\Psi|^2$ at time t as

$$P(|\Psi|^2, t) = \frac{W(|\Psi|^2, t) - W(|\Psi|^2 + \Delta A, t)}{\Delta A}, \quad (12)$$

where $W(Y, t)$ is the ensemble average probability to meet squared amplitude $|\Psi|^2$ larger than Y , and $\Delta A = 0.1$ is the bin size. Since $\int F(x)x dx = (1/2) \int F(x) dx^2$, the PDF to meet squared amplitude $|\Psi|^2$ is exponential if the corresponding amplitude PDF $P(|\Psi|)$ is Rayleigh one,

$$P_R(|\Psi|^2) = \frac{1}{\sigma^2} \exp(-|\Psi|^2/\sigma^2). \quad (13)$$

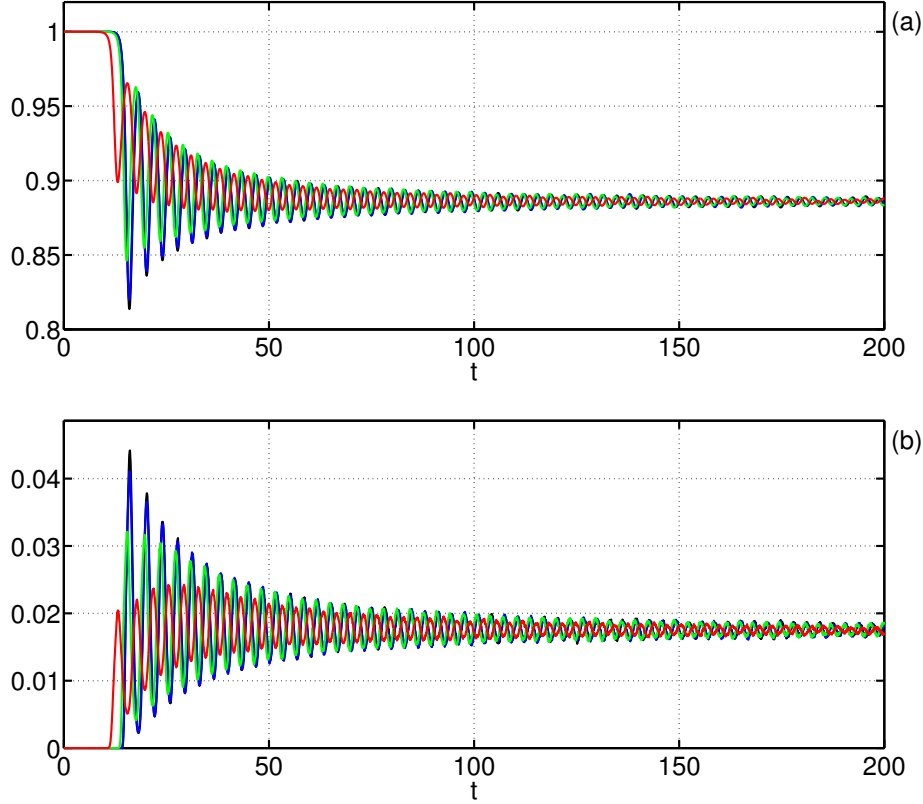


FIG. 5. (Color on-line) Evolution of the generalized mean $M^{(1)}(t)$ (a) and the squared amplitude PDF $P(|\Psi|^2, t)$ at $|\Psi|^2 = 4$ (b) for noise parameters $A_0 = 10^{-6}$, $\theta = 5$ (black), $A_0 \approx 1.17 \times 10^{-6}$, $\theta = 1$ (blue), $A_0 \approx 1.66 \times 10^{-5}$, $\theta = 0.5$ (green) and $A_0 \approx 8.92 \times 10^{-4}$, $\theta = 0.35$ (red). During these experiments noise amplitude in k -space at $|k| = 1$ was fixed to $q_0 = A_0 \left(\frac{L\sqrt{8\pi}}{\theta} \right)^{1/2} \exp(-1/\theta^2) \approx 2.73 \times 10^{-5}$.

As in [9], we observe the squared amplitude PDFs $P(|\Psi|^2, t)$ that in the nonlinear stage of the modulation instability are close to exponential form (13) with $\sigma = 1$, though time-dependent deviations from this form are visible up to $t \sim 50$ (see FIG. 4).

When we fix squared amplitude $|\Psi|^2$ and study the time dependence of the PDF, we observe exactly the same behavior as written above for the generalized means: the PDF $P(|\Psi|^2, t)$ oscillates around the Rayleigh PDF (13) with $\sigma = 1$, so that the asymptotic PDF calculated by averaging $P(|\Psi|^2, t)$ over time $t \in [150, 200]$ coincides with (13) with $\sigma = 1$. The amplitude of these oscillations decay with time as $t^{-3/2}$, and the phase of the oscillations contain the nonlinear phase shift that decays as $t^{-1/2}$. These oscillations evolve in-phase with $M^{(1)}(t)$ for $|\Psi|^2 \lesssim 2$ and antiphase with $M^{(1)}(t)$ for $|\Psi|^2 \gtrsim 2$, and overall are very well approximated by the ansatz (10), as shown on FIG. 3b for the case $|\Psi|^2 = 4$.

However, we are able to track down such oscillations only up to $|\Psi|^2 = 6$; beyond this threshold our output results resemble random noise. We think that this situation occurs because beyond $|\Psi|^2 \sim 6$ the law of how the PDF evolves with time changes. Indeed, as shown

on FIG. 4 on the example of the PDFs corresponding to $t = 14$, $t = 16$, $t = 18$ and $t = 100$, for $|\Psi|^2 > 7$ the PDF does not fluctuates around the Rayleigh PDF (13), but rather approaches to it from below.

IV. DEPENDENCE ON STATISTICS OF INITIAL NOISE.

We repeated our experiments for ensembles of initial data with different noise parameters. We didn't find significant dependence of our results on noise amplitude A_0 , except that with decreasing of A_0 , the time necessary for the nonlinear stage of the MI to arrive increases. The period of the oscillations $\Delta T = 2\pi/b \approx \pi$ does not depend on A_0 , and the oscillations start roughly with the same amplitudes for all of our experiments from $A_0 = 10^{-12}$ to $A_0 = 10^{-3}$.

We also tested the following noise distribution,

$$\epsilon_2(x) = A_0 \left(\frac{L\sqrt{8\pi}}{\theta} \right)^{1/2} \times$$

$$\times \int 10^{-p_k} e^{-k^2/\theta^2 + i\xi_k + ikx} \frac{dk}{2\pi}, \quad (14)$$

where p_k is uniformly distributed over $[0, 10]$ random value for each k , $A_0 = 10^{-5}$ and $\theta = 5$. The multiplier 10^{-p_k} introduces the detuning between the amplitudes of noise in k -space by up to 10 orders of magnitude. However, we came to very similar results, though the oscillations became less regular. In our opinion this means that the oscillations we observe should be visible for a very wide variety of statistical distributions of noise.

The most significant dependence of our results was found on the noise width in k -space θ . We performed four experiments changing θ from $\theta = 5$ to $\theta = 0.35$. During these experiments we fixed noise amplitude at $|k| = 1$ to

$$q_0 = A_0 \left(\frac{L\sqrt{8\pi}}{\theta} \right)^{1/2} \exp(-1/\theta^2) \approx 2.73 \times 10^{-5},$$

so that $A_0 = 10^{-6}$ for $\theta = 5$. As $|k| = 1$ is the fastest growing mode in the linear stage of the MI, and assuming that at the start of the nonlinear stage this mode is the leading one after the zeroth harmonic $k = 0$, such condition should provide us the same starting time for the nonlinear stage of the MI for the experiments with different θ . This supposition turns out to be valid for the experiment with $A_0 = 1.17 \times 10^{-6}$, $\theta = 1$, when all of the functions that we measure, including the generalized means, the PDFs, the energy spectrum and the spacial correlation functions (see [9] for more information), almost coincide with that for the experiment with noise parameters $A_0 = 10^{-6}$, $\theta = 5$. However, for the experiments with $A_0 = 1.66 \times 10^{-5}$, $\theta = 0.5$ and $A_0 = 8.92 \times 10^{-4}$,

$\theta = 0.35$ we observe significantly different results than before.

As shown on FIG. 5, the oscillations became non-symmetric with respect to the asymptotic values of the oscillating functions at large times, however, these asymptotic values still coincide with the Rayleigh predictions. The amplitudes of the oscillations became smaller, and the local maximums and the local minimums of the oscillating functions belong now to different time dependencies. However, for local maximums of $M^{(1)}(t)$ and $P(|\Psi|^2, t)$ at $|\Psi|^2 \lesssim 2$, and local minimums of $M^{(n)}(t)$, $n \geq 3$, and $P(|\Psi|^2, t)$ at $|\Psi|^2 \gtrsim 2$, we still observe the decay of the amplitude of the oscillations as $\sim t^{-3/2}$. The period of the oscillations $\Delta T = 2\pi/b \approx \pi$ also does not change with θ .

V. ACKNOWLEDGEMENTS.

D. Agafontsev thanks E. Kuznetsov for valuable discussions concerning the subject of this publication, M. Fedoruk for access to and V. Kalyuzhny for assistance with Novosibirsk Supercomputer Center. This work was done in the framework of Russian Federation Government Grant (contract No. 11.G34.31.0035 with Ministry of Education and Science of RF), and also supported by the program of Presidium of RAS "Fundamental problems of nonlinear dynamics in mathematical and physical sciences", program of support for leading scientific schools of Russian Federation, RFBR grants 12-01-00943-a, 13-01-00261 and also Sergei Badulin RFBR grant 11-05-01114-a.

-
- [1] T.B. Benjamin, J.E. Feir, *The disintegration of wave trains on deep water Part 1. Theory*, J. Fluid Mech., vol. 27, part 3, pp. 417-430 (1967).
 - [2] V.E. Zakharov, *Stability of periodic waves of finite amplitude on the surface of a deep fluid*, Zh. Prikl. Mekh. Tekh. Fiz. 9, 86-94 (1968) [J. Appl. Mech. Tech. Phys. 9, 190-194 (1968)].
 - [3] V.E. Zakharov, S.V. Manakov, S.P. Novikov, L.P. Pitaevsky, *Theory of solitons. The method of the inverse scattering problem*, Consultants Bureau, New York (1984).
 - [4] D.H. Peregrine, *Water waves, nonlinear Schrodinger equations and their solutions*, J. of the Australian Math. Soc. B, vol. 25, iss. 01, pp. 16-43 (1983).
 - [5] G.P. Agrawal, P.L. Kelley, I.P. Kaminow, *Nonlinear Fiber Optics*, 3rd ed. Academic, San Diego (2001).
 - [6] P.A. Ruprecht, M.J. Holland, K. Burnett, M. Edwards, *Time-dependent solution of the nonlinear Schrodinger equation for Bose-condensed trapped neutral atoms*, Phys. Rev. A 51, 4704 (1995).
 - [7] E.A. Kuznetsov, *Solitons in a parametrically unstable plasma*, Sov.Phys. - Dokl. (Engl. Transl.) vol. 22, 507 (1977) [*On solitons in parametrically unstable plasma*, Doklady USSR (in Russian) vol. 236, 575 (1977)].
 - [8] V.E. Zakharov, A.A. Gelash, *Nonlinear Stage of Modulation Instability*, Phys. Rev. Lett. 111, 054101 (2013).
 - [9] D.S. Agafontsev, V.E. Zakharov, *Rogue waves statistics in the framework of one-dimensional Generalized Nonlinear Schrodinger Equation*, arXiv:1202.5763v3 (2012).
 - [10] G.M. Muslu, H.A. Erbay, *Higher-order split-step Fourier schemes for the generalized nonlinear Schrodinger equation*, Mathematics and Computers in Simulation, v. 67, iss. 6 (2005).
 - [11] R.I. McLachlan, *On the numerical integration of ordinary differential equations by symmetric composition methods*, SIAM Journal on Scientific Computing, v. 16, iss. 1 (1995).
 - [12] D.S. Agafontsev, *Waves statistics for generalized one-dimensional Nonlinear Schrodinger Equation with saturated nonlinearity*, arXiv:1310.3618 (2013).